Resonance States of Negative Hydrogen-like Ions in Quantum Plasmas

Suya Yao [1], **Zishi Jiang** [1,*] **and Sabyasachi Kar** [2]

1 College of Physical Science and Technology, Heilongjiang University, Harbin 150080, China; yaosy230221@163.com
2 School of Physics, Harbin Institute of Technology, Harbin 150001, China; skar@hit.edu.cn
* Correspondence: jiangzishi@hlju.edu.cn

Abstract: We studied the $^1S^e$ and $^{1,3}P^o$ resonance states of negative hydrogen-like ions immersed in quantum plasmas. The exponential cosine screened Coulomb potential was considered to model the quantum plasma environment. The correlated exponential wave functions in which the exponents were generated by a pseudo-random technique were applied to represent the correlation effects between the charged particles. The stabilization method was used to calculate the resonance parameters (position and width). The resonance parameters (position and width) for Ps^-, $M\mu^-$, π^-, $^1H^-$, D^-, T^- and $^\infty H^-$ embedded in quantum plasmas are reported for various screening parameters. The $^1S^e$ resonance parameters for $M\mu^-$, π^-, $^1H^-$, D^-, T^- ions and $^{1,3}P^o$ states for Ps^-, $M\mu^-$, π^-, $^1H^-$, D^-, T^- and $^\infty H^-$ of the proposed systems are reported for the first time in the literature.

Keywords: resonance states; correlated exponential wave functions; stabilization method; quantum plasmas

1. Introduction

The study of the resonance states of two-electron negative ions is of great theoretical and experimental importance because negative ions are very sensitive to electron–electron correlations. The theoretical and experimental studies of $^1S^e$ and $^{1,3}P^o$ resonance states in two-electron anions involve mainly the two simplest examples, namely, the negative hydrogen ions ($^\infty H^-$) and the positronium negative ion (Ps^-). The Ps^- is a simple three-lepton system, predicted theoretically by Wheeler [1] and observed (Ps^- is formed by a 420 eV positron beam striking a thin film of carbon in a vacuum [2,3]) in the laboratory by Mills [2,3]. After the first prediction of this ion, several studies have been reported on this simplest three-body system. In addition to extensive theoretical studies of the resonance states [4–18], physicists have also made experimental observations [19–23] about resonance. New developments in the field of Ps^- effective emission experiments on alkali metal coated-surfaces were recently highlighted in a review article by Nagashima [20,22,24] and Mills [21]. Notably, the first and only experiment on a shape resonance state was reported by Michishio et al. [23].

It is well known that hydrogen negative ions ($^\infty H^-$) are the main source of continuous opacity in the solar photosphere. Over the last few decades, many researchers have made considerable efforts to investigate theoretically the resonance state of $^\infty H^-$ using different sophisticated methods or techniques [25–36]. From the experimental side, Hamm and colleagues [37–40] reported the observation of $^\infty H^-$ resonance states, and recent experimental progress has been summarized in a review [41].

Negative ions having two electrons, in particular, Ps^-, $M\mu^-$, π^-, $^1H^-$, D^-, T^- as well as $^\infty H^-$, have a very simple bound-state spectrum, which contains only one bound state (ground state) with a single $1s^2\ ^1S$ state with total angular momentum $L = 0$. The stability of μ^- has been known for a long time since its discovery by Kuang [42]. Subsequently, the bound state nature of this elusive negative ion was reported by Frolov et al. [43–46]. The

resonance states of two-electron negative ions have been theoretically investigated so far based on the complex coordinate rotation method [18,35,36], the variational method [25, 33], the stabilization method [17], the close coupling method [13,14,29,31], the adiabatic molecular approximation [6,10], the R-matrix [27], etc. In addition to the theoretical and experimental progress made for the unscreened case, resonance states of two-electron systems have also been studied theoretically in a screening environment [47–56].

In addition, P. K. Shukla et al. [57] found that the exponential cosine screened Coulomb potential (ECSCP) can better model the effective electron-ion potential in a dense quantum plasma, expressed in terms of the screening parameter λ as:

$$V(r) = \frac{1}{r} e^{-\lambda r} cos(\lambda r) \tag{1}$$

where the screening parameter λ is related to the frequency of the plasma and satisfies the relation: $\lambda = \omega_p / (\hbar \omega_p / m)^{1/2}$. The screening parameters λ determine the screening effect, and as the screening parameters increase, the screening also increases. ECSCP plays a fundamental role in the study of atomic structures and collisions in quantum plasmas and has the advantage that it exhibits a stronger screening effect than the screening Coulomb potential due to the presence of an oscillatory part (the cosine term in the potential). It can become a pure Coulomb potential when the screening parameter λ becomes zero. Ghoshal et al. pioneered a theoretical study of the nature of the interaction of Ps^- [58,59] and H_2^+ [60] with ECSCP and reported precise results for the S-wave resonance state of $^\infty H^-$ [61] in the ECSCP using the stabilization method. Kar and Ho [62] described the effects on various properties of Ps^- within the ECSCP.

In the present work, we studied the $^1S^e$ and $^{1,3}P^o$ resonance states of negative hydrogen-like ions embedded in quantum plasma environments. The $^1S^e$ and $^{1,3}P^o$ resonance states are affected by the screening environment in which the Coulomb potential is replaced by an exponential cosine screened Coulomb potential. Using a correlated exponential wave function within the framework of the stabilization method, we determined the precise values of the resonance parameters (position and width) for the different screening parameters. In this paper, we report the resonance parameters of each ionic system lying below the $N = 2$ threshold of the respective subsystem. To our knowledge, such resonance states have not been reported previously for the exponential cosine screened Coulomb potential. The plan of this paper is as follows: Section 2 describes the basic computational aspects of the study; Section 3 presents the results and discussion in connection with our calculations; in Section 4, we present the conclusions of the study. Atomic units (a.u.) are used throughout the work.

2. Theory

The non-relativistic Hamiltonian describing a two-electron negative ion system in a screening environment is:

$$H = -\frac{1}{2}\nabla_1^2 - \frac{1}{2}\nabla_2^2 - \frac{1}{2M}\nabla_3^2$$

$$- \frac{exp(-\lambda r_{31})}{r_{31}} cos(\lambda r_{31}) - \frac{exp(-\lambda r_{32})}{r_{32}} cos(\lambda r_{32}) + \frac{exp(-\lambda r_{12})}{r_{12}} cos(\lambda r_{12}) \tag{2}$$

where 1, 2 and 3 represent the two electrons 1, 2 with the nucleus, respectively, and r_{ij} represents the relative distance between the two particles. The mass constants M_μ, M_{1_H}, M_D, M_T and M_π used in this paper were $206.7682826m_e$, $1836.15267389m_e$, $3670.48296785m_e$, $5496.92153588m_e$ [63] and $273.132426m_e$ [64].

For the S and P states, we considered an exponential wave function of the following form to describe the system:

$$\Psi = \left(1 + S_{pn}\hat{P}_{12}\right) \sum_{i=1}^{N} C_i r_1^L P_L(cos\theta_1) exp[(-\alpha_i r_{31} - \beta_i r_{32} - \gamma_i r_{12})\omega] \tag{3}$$

In the above equation, $C_i (i = 1, \ldots, N)$ is the linear expansion coefficient; α_i, β_i, γ_i are the linear variational parameters; ω is a scaling constant; N is the number of basis function terms, and the operator $\hat{P}_{12}$ denotes the exchange of two particles marked 1 and 2, i.e.: $\hat{P}_{12} f(r_1, r_2, r_{12}, \theta_1) = f(r_2, r_1, r_{12}, \theta_2)$. $L = 0$ for the S-state, $L = 1$ for the P-state. $S_{pn} = 1$ for the singlet state, $S_{pn} = -1$ for the triplet state. The nonlinear parameters α_i, β_i, γ_i in the wave function formulation were chosen from three positive intervals, i.e., $[A_1^{(k)}, A_2^{(k)}]$, $[B_1^{(k)}, B_2^{(k)}]$ and $[C_1^{(k)}, C_2^{(k)}]$, where $k = \mod(i, 3) + 1$, $1 \leq i \leq N$, following a pseudorandom technique [65]

$$\alpha_i = \eta_1^{(k)} \left[\langle\langle \frac{1}{2} i(i+1)\sqrt{2} \rangle\rangle \left(A_2^{(k)} - A_1^{(k)} \right) + A_1^{(k)} \right],$$

$$\beta_i = \eta_2^{(k)} \left[\langle\langle \frac{1}{2} i(i+1)\sqrt{3} \rangle\rangle \left(B_2^{(k)} - B_1^{(k)} \right) + B_1^{(k)} \right], \tag{4}$$

$$\gamma_i = \eta_3^{(k)} \left[\langle\langle \frac{1}{2} i(i+1)\sqrt{5} \rangle\rangle \left(C_2^{(k)} - C_1^{(k)} \right) + C_1^{(k)} \right],$$

where the symbol $\langle\langle \cdots \rangle\rangle$ denotes the fractional part of a real number; $\eta_1^{(k)}$, $\eta_2^{(k)}$, $\eta_3^{(k)}$ are scaling factors, $A_1^{(k)} = 0$, $A_2^{(k)} = a$, $B_1^{(k)} = 0$, $B_2^{(k)} = b$, $C_1^{(k)} = 0$, $C_2^{(k)} = c$, $\eta_1^{(k)} = 1$, $\eta_2^{(k)} = 1$ and $\eta_3^{(k)} = \lambda$. In the course of theoretical numerical calculations, good results can be obtained by the optimal choice of these parameters.

Regarding the calculation of the resonant states, we used the stabilization method proposed by Mandelshtam et al. [66] and later developed by Ho [67] for atomic resonance calculations, which is a powerful method for calculating atomic resonances. The advantage of this method is that it requires neither the use of a complex analytic extension nor the solution of the scattering function, and only the L^2 function is needed to calculate resonance energy and width, which is a simple and efficient alternative in the field of atomic resonance calculations. In the first step to exploit the stabilization method, we diagonalized Hamiltonian $\hat{H}(2)$ using the wave function (3) to calculate the corresponding energy level $E(\omega)$. We then plotted a steady-state diagram (see Figures 1a and 2a) of $E(\omega)$ as a function of ω. Smooth or slowly decreasing energy levels in the diagram indicate the location of the resonance at energy E. In order to extract the specific resonance parameter (E_r, Γ), the density of the resonance states for each single energy level in the stable plateau needs to be calculated by applying the following equation:

$$\rho_n(E) = \left| \frac{E_n(\omega_{i+1}) - E_n(\omega_{i-1})}{\omega_{i+1} - \omega_{i-1}} \right|^{-1}_{E_n(\omega_i) = E} \tag{5}$$

where index i denotes the ith value of ω, and the index n denotes the nth level of the resonance.

After calculating the resonance density of the states $\rho_n(E)$ by the above equation, we fit it to the following Lorentzian form to obtain the resonant energy E_r and the resonant width Γ:

$$\rho_n(E) = y_0 + \frac{A}{\pi} \frac{\dfrac{\Gamma}{2}}{(E - E_r)^2 + \left(\dfrac{\Gamma}{2} \right)^2} \tag{6}$$

where y_0 is the baseline offset, A is the total area between the curve down to the baseline, E_r represents the centre of the peak, and Γ indicates the full width of the curve peak at half height. When fitting in Lorentzian form, the best fit (closest to 1.0), the ideal result for a particular resonance, can be determined by observing the minimum value of χ^2 and the best value of r^2, the square of the correlation coefficients (see Figures 1b and 2b).
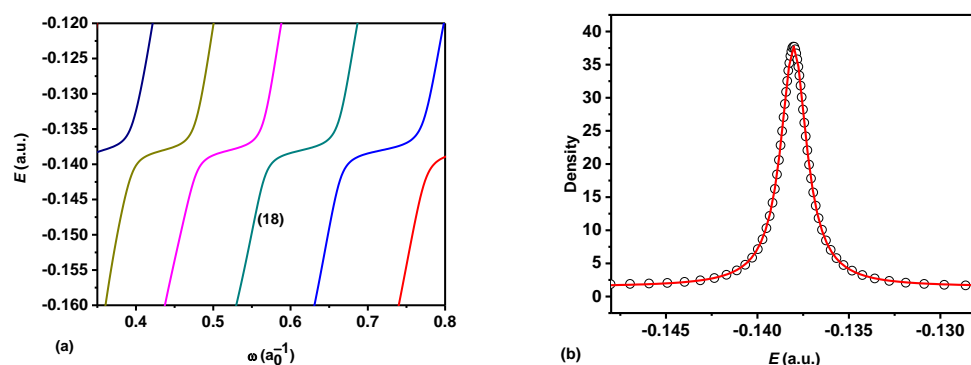
Figure 1. (**a**) Stabilization diagram for the $^1S^e$ state of $M\mu^-$ at $\lambda = 0.01$ (the number 18 in the diagram indicates the 18th energy level). (**b**) Calculated densities (circles) and Lorentzian fits (solid line and the best fit) for the $^1S^e$ state of $M\mu^-$ at $\lambda = 0.01$.
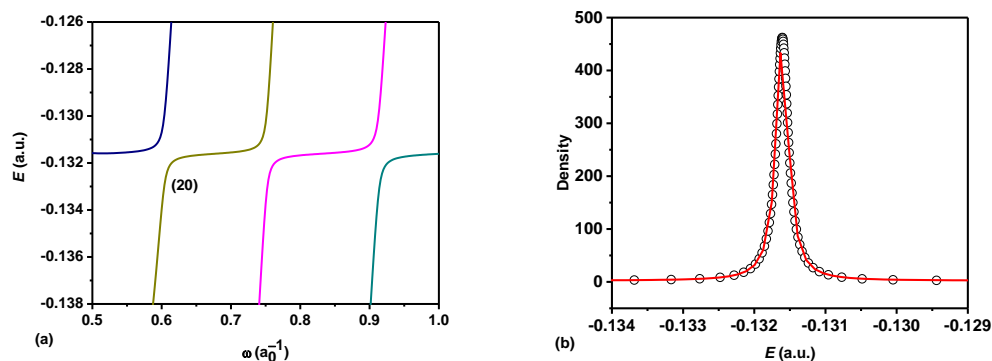
Figure 2. (**a**) Stabilization diagram for the $^3P^o(1)$ state of π^- for $\lambda = 0.01$ (the number 20 in the diagram indicates the 20th energy level). (**b**) Calculated densities (circles) and Lorentzian fits (solid line and the best fit) for the $^3P^o(1)$ state of π^- for $\lambda = 0.01$.

3. Results and Discussion

By taking advantage of the stabilization method, we calculated the resonance parameters (RPs) for the $^1S^e$ and $^{1,3}P^o$ states of negative hydrogen-like ions interacting with ECESCP. The resonance energies and widths for the systems Ps^-, $M\mu^-$, π^-, $^1H^-$, D^-, T^- and $^\infty H^-$ are presented in Tables 1–6 in terms of screening parameters. In Figures 1 and 2, the stabilization diagram and the best fitting of the density of the resonance states for the systems $M\mu^-$ and π^- are displayed. We calculated the density of the resonant states for a single energy level in the range 0.3 to 1.0 of ω. Figures 1b and 2b show, respectively, the best fit of the density of the resonant states corresponding to the 18th and 20th energy levels in the stabilization plateau in Figures 1a and 2a. From the fittings, we obtained the resonance energy $E_r = -0.1380189(a.u.)$ and resonance width $\Gamma = 1.712 \times 10^{-3}(a.u.)$ in the $^1S^e$ state of $M\mu^-$ under the screening parameter $\lambda = 0.01$, and the resonance energy $E_r = -0.1316061(a.u.)$ and resonance width $\Gamma = 2.044 \times 10^{-4}(a.u.)$ in the $^3P^o(1)$ state of π^- under the screening parameter $\lambda = 0.01$. By changing the value of λ, the RPs for different effective parameters and different ionic systems were obtained.

Tables 1 and 2 provide the RPs of seven ions from Ps^- to H^- in the lowest $^1S^e$ state for different screening parameters. The S^e state RPs for Ps^- and $^\infty H^-$ for different screening parameters were comparable with the previously published data by Ghoshal and Ho [59,61]. Tables 3 and 4 display the resonance parameters of seven ions from Ps^- to $^\infty H^-$ in the lowest $^3P^o$ state under different screening parameters. The lowest $^1P^o$ state RPs for the proposed systems are listed in Tables 5 and 6. When the system was in an unscreened environment, i.e., $\lambda = 0$, the interaction potential turned into a Coulomb potential. For Ps^- and $^\infty H^-$, the results calculated by us were comparable to those in published reports; the comparisons are presented in Tables 3 and 4. It is of special interest to mention here

that the $^1S^e$ resonance parameters for the system $^\infty H^-$ were in good accord with reported results by Ho et al. [68].

According to Tables 1–6, the resonance energy E_r and the resonance width Γ of the $^1S^e$ and $^{1,3}P^o$ states of each ionic system and the threshold energy of respective subsystem changed with an increasing λ. It is important to note here that, because of the structure of the different systems, the positively charged particles of the systems had different masses. It can be clearly seen in Figures Figures 3a–16a, that the resonance energy E_r of the system tended to the threshold of the corresponding single-electron subsystem with the increase of the screening parameter λ. For the $^1S^e$ state, the systems approached the respective thresholds when the screening parameter λ was about $0.16a_0^{-1}$, except for the system Ps^- which approached the threshold energy at $\lambda = 0.1a_0^{-1}$. The value of λ for which the resonance energy of a system approaches the threshold energy of the respective subsystem is referred as the critical value. For the $^3P^o$ state, the critical value of λ was about 0.07 for Ps^-, and for the other systems, the critical value of λ was about 0.12. For the $^1P^o$ state, the critical value of λ was about 0.02 for Ps^-, and for the other systems, the critical value of λ was about 0.03. As can be seen in Figures 3b–16b, for a weak screening effect, the resonance width Γ slowly increased with the increase of the screening parameter λ, and then λ began to decease rapidly. The resonance energy of the $^1S^e$ and $^{1,3}P^o$ states of the two-electron negative ion system was calculated for $N = 700$ and $N = 600$, respectively.

In the Tables and Figures, we can observe that the lowest $^1S^e$ and $^{1,3}P^o$ resonance parameters (E_r, Γ) from Ps^- to $^\infty H^-$ interacting with ECSCP changed with nuclear masses m and screening parameter λ. It can be seen in Tables 1, 3 and 5 that the resonance energy E_r gradually decreased with the increase of the system mass m. For a particular ion, the resonance energy and the threshold energy also increased with the increase of the screening parameter. This is because the ionic system needed more energy to become free from plasma bonding with an increasing screening strength. In addition, the resonance width Γ gradually increased with the increase of the nuclear mass, and all showed an overall trend for the resonance width, which first increased slowly with the increase of the shielding parameter and then began to rapidly decrease. The physical interpretation of the increasing and decreasing trends of the resonance widths for negative hydrogen-like ions has been well described in previous articles [48,51,52,58,61]. It is interesting to note the range of the screening parameter λ, which supports a resonance state for a particular ionic system embedded in quantum plasmas. For Ps^-, the ranges of λ were $0 < \lambda \le 0.08$, $0 < \lambda \le 0.07$ and $0 < \lambda \le 0.02$ for the lowest $^1S^e$, $^3P^o$ and $^1P^o$ states, respectively. For all other ionic systems, the ranges of the screening parameter λ were $0 < \lambda \le 0.16$, $0 < \lambda \le 0.12$ and $0 < \lambda \le 0.03$ for the lowest $^1S^e$, $^3P^o$ and $^1P^o$ states, respectively.

Finally, we would like to mention the importance of our work in an astrophysical context. It is well documented in the literature that the opacity of the atmosphere of the Sun depends on several processes such as Thomson scattering, bound–bound transitions, and the photodetachment (bound–free) of hydrogen and positronium ions. For details on the bound-bound and bound-free transitions of $^\infty H^-$ and Ps^- in the unscreened case, the interested readers are referred to the recent review article by Bhatia and Pesnell [69]. For the screened case, the photodetachment of $^\infty H^-$ and Ps^- has also been reported in the literature [50,70,71]. In the present study, we present the effects of ECSCP on the resonance parameters for different resonance states of negative hydrogen-like ions. It is also important to point out here that the appropriateness of quantum screening potentials for negative hydrogen-like ions has been well discussed in previously published articles [50–63,70–73]. Our findings might be useful for further studies on this topic.

Table 1. $^1S^e$ resonance energies E_r (a.u.) of two-electron negative ions for different values of the screening parameter λ.

λ	Ps$^-$	Mμ^-	π^-	^{1}H$^-$	D$^-$	T$^-$	∞H$^-$
0.00	−0.0760300 −0.076030 [a]	−0.1480453	−0.1482105	−0.1486748	−0.1487155	−0.1487291	−0.1487563 −0.14876 [b]
0.01	−0.0659912 −0.065992 [a]	−0.1380189	−0.1381932	−0.1386573	−0.1386983	−0.1387119	−0.1387391 −0.13875 [b]
0.02	−0.0558114 −0.055812 [a]	−0.1279178	−0.1280922	−0.1285570	−0.1285977	−0.1286113	−0.1286385 −0.12865 [b]
0.03	−0.0455464	−0.1176989	−0.1178735	−0.1183388	−0.1183796	−0.1183932	−0.1184205
0.04	−0.0353743	−0.1073700	−0.1075448	−0.1080105	−0.1080513	−0.1080649	−0.1080922
0.05	−0.0255309 −0.025531 [a]	−0.0969679	−0.0971426	−0.0976082	−0.0976082	−0.0976626	−0.0976899 −0.09770 [b]
0.06	−0.0162967	−0.0865485	−0.0867227	−0.0871872	−0.0872279	−0.0872414	−0.0872686
0.07	−0.0080506	−0.0761792	−0.0763524	−0.0768141	−0.0768545	−0.0768680	−0.0768951
0.08	−0.0015421	−0.0659352	−0.0661066	−0.0665635	−0.0666035	−0.0666168	−0.0666436
0.09		−0.0558972	−0.0560658	−0.0565152	−0.0565546	−0.0565677	−0.0565941
0.10		−0.0461518	−0.0463163	−0.0467549	−0.0467934	−0.0468062	−0.0468319
0.11		−0.0367941	−0.0369530	−0.0373767	−0.0374139	−0.0374263	−0.0374512
0.12		−0.0279338	−0.0280850	−0.0284885	−0.0285240	−0.0285357	−0.0285594
0.13		−0.0197075	−0.0198483	−0.0202241	−0.0202571	−0.0202681	−0.0202902
0.14		−0.0123046	−0.0124305	−0.0127674	−0.0127970	−0.0128068	−0.0128267
0.15		−0.0060262	−0.0061298	−0.0064081	−0.0064327	−0.0064408	−0.0064573
0.16		−0.0013941	−0.0014624	−0.0016483	−0.0016649	−0.0016704	−0.0016815

[a] Ref. [59]. [b] Ref. [61].

Table 2. $^1S^e$ resonance widths $\Gamma\left(\times 10^{-3}\right)$ (a.u.) of negative hydrogen-like ions for different screening values of the parameter λ.

λ	Ps$^-$ (10^{-5})	Mμ^-	π^-	^{1}H$^-$	D$^-$	T$^-$	∞H$^-$
0.01	4.303 4.30 [a]	1.700	1.716	1.730	1.732	1.732	1.733 1.732 [b]
0.01	4.321 4.32 [a]	1.712	1.717	1.730	1.731	1.732	1.733 1.733 [b]
0.02	4.400 4.41 [a]	1.717	1.721	1.736	1.737	1.737	1.738 1.738 [b]
0.03	4.516	1.725	1.730	1.744	1.745	1.745	1.746
0.04	4.599	1.734	1.740	1.753	1.755	1.755	1.756
0.05	4.549 4.54 [a]	1.741	1.747	1.761	1.762	1.762	1.763 1.764 [b]
0.06	4.231	1.741	1.746	1.760	1.762	1.762	1.763
0.07	3.422	1.729	1.734	1.748	1.750	1.750	1.751
0.08	1.662	1.699	1.704	1.719	1.720	1.721	1.722
0.09		1.647	1.653	1.668	1.669	1.669	1.700
0.10		1.567	1.573	1.589	1.590	1.591	1.592
0.11		1.456	1.462	1.478	1.479	1.480	1.481
0.12		1.304	1.311	1.327	1.329	1.329	1.330
0.13		1.104	1.111	1.128	1.130	1.131	1.130
0.14		0.840	0.848	0.867	0.869	0.869	0.871
0.15		0.498	0.506	0.527	0.529	0.530	0.531
0.16		0.149	0.154	0.167	0.169	0.169	0.170

[a] Ref. [59]. [b] Ref. [61].

Table 3. $^3P^o$ resonance energies E_r (a.u.) of negative hydrogen-like ions immersed in a quantum plasma environment for different values of the screening parameter λ.

λ	Ps$^-$	Mμ^-	π^-	^{1}H$^-$	D$^-$	T$^-$	∞H$^-$
0.00	−0.0733263 −0.07332659 [a]	−0.1414591	−0.1416224	−0.1420576	−0.1420958	−0.1421084	−0.1421340 −0.142133 [b]
0.01	−0.0632875	−0.1314427	−0.1316061	−0.1320414	−0.1320795	−0.1320922	−0.1321177
0.02	−0.0531113	−0.1213487	−0.1215121	−0.1219477	−0.1219859	−0.1219986	−0.1220242
0.03	−0.0428660	−0.111149	−0.1113123	−0.1117484	−0.1117866	−0.1117993	−0.1118249
0.04	−0.0327415	−0.1008551	−0.1010189	−0.1014555	−0.1014937	−0.1015064	−0.1015320
0.05	−0.0229806	−0.0905085	−0.0906723	−0.0911086	−0.0911469	−0.0911596	−0.0911852
0.06	−0.0138667	−0.0801663	−0.0803296	−0.0807647	−0.0808028	−0.0808155	−0.0808410
0.07	−0.0058038	−0.0698958	−0.0700580	−0.0704903	−0.0705282	−0.0705408	−0.0705662
0.08		−0.0597701	−0.0599304	−0.0603578	−0.0603953	−0.0604078	−0.0604329
0.09		−0.0498661	−0.0500237	−0.0504437	−0.0504805	−0.0504928	−0.0505174
0.10		−0.0402659	−0.0404195	−0.0408288	−0.0408647	−0.0408767	−0.0409007
0.11		−0.0310604	−0.0312083	−0.0316030	−0.0316376	−0.0316491	−0.0316723
0.12		−0.0223635	−0.0225036	−0.0228775	−0.0229103	−0.0229212	−0.0229432

[a] Ref. [48]. [b] Ref. [56].

Table 4. $^3P^o$ resonance widths $\Gamma\left(\times 10^{-4}\right)$ (a.u.) of hydrogen-like ionic systems for different values of the screening parameter λ.

λ	Ps$^-$	Mμ^-	π^-	^{1}H$^-$	D$^-$	T$^-$	∞H$^-$
0.00	1.282 1.274 [a]	2.009	2.043	2.136	2.144	2.146	2.152 2.14 [b]
0.01	1.287	2.010	2.044	2.137	2.145	2.148	2.153
0.02	1.308	2.017	2.051	2.144	2.152	2.155	2.161
0.03	1.330	2.031	2.066	2.159	2.167	2.170	2.175
0.04	1.325	2.049	2.084	2.177	2.186	2.188	2.194
0.05	1.260	2.067	2.102	2.196	2.204	2.207	2.213
0.06	1.097	2.079	2.114	2.208	2.217	2.219	2.225
0.07	0.7683	2.079	2.114	2.208	2.216	2.219	2.225
0.08		2.060	2.095	2.188	2.196	2.199	2.204
0.09		2.015	2.049	2.140	2.148	2.151	2.156
0.10		1.935	1.967	2.056	2.063	2.066	2.071
0.11		1.806	1.837	1.921	1.928	1.931	1.936
0.12		1.601	1.629	1.708	1.715	1.718	1.723

[a] Ref. [48]. [b] Ref. [56].

Table 5. $^1P^o$ resonance energies E_r (a.u.) of two-electron negative ions for different values of λ.

λ	Ps$^-$	Mμ^-	π^-	^{1}H$^-$	D$^-$	T$^-$	∞H$^-$
0.00	−0.06315584	−0.1254399	−0.1255875	−0.1259808	−0.1260153	−0.1260268	−0.1260498
0.01	−0.05306434	−0.1153986	−0.1155463	−0.1159398	−0.1159743	−0.1159858	−0.1160089
0.02	−0.04293079	−0.1052296	−0.1053774	−0.1057712	−0.1058057	−0.1058172	−0.1058402
0.03		−0.09502556	−0.09517295	−0.09556560	−0.09560001	−0.09561146	−0.09563447

Table 6. $^1P^o$ resonance widths $\Gamma\left(\times 10^{-6}\right)$ (a.u.) of two-electron negative ions for different values of λ.

λ	Ps$^-$	Mμ^-	π^-	^{1}H$^-$	D$^-$	T$^-$	∞H$^-$
0.00	0.9132	1.452	1.443	1.421	1.419	1.418	1.417
0.01	1.297	1.534	1.525	1.500	1.497	1.497	1.495
0.02	2.902	2.095	2.081	2.043	2.039	2.038	2.036
0.03		3.418	3.397	3.343	3.338	3.336	3.333
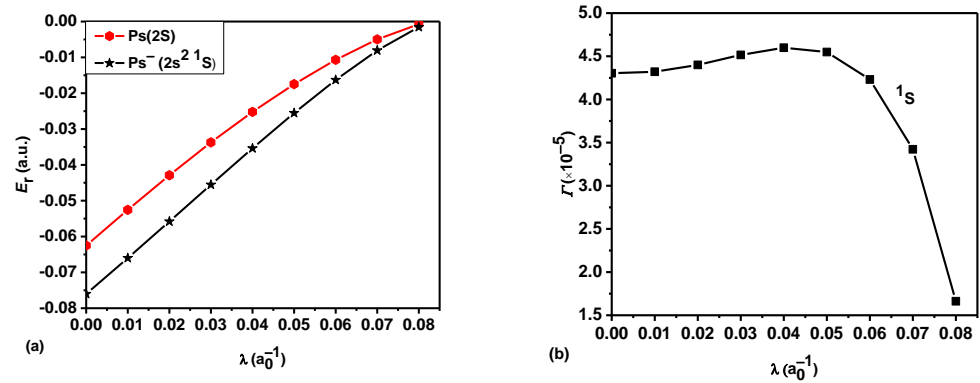
Figure 3. (**a**) Plot of the lowest $^1S^e$ resonance energy E_r of Ps$^-$ as a function of λ. (**b**) Plot of the resonance corresponding resonance width Γ of Ps$^-$ as a function of λ.
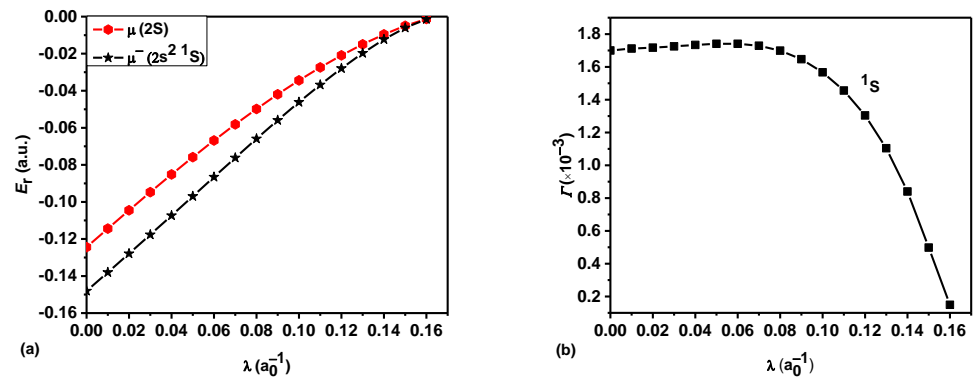
Figure 4. (**a**) Plot of the lowest $^1S^e$ resonance energy E_r of Mμ^- vs. the screening parameter λ. (**b**) Plot of the resonance width Γ of Mμ^- vs. the screening parameter λ.
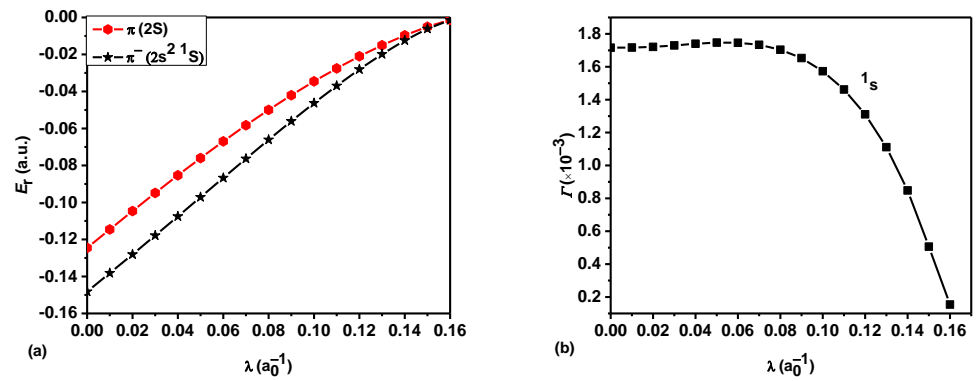
Figure 5. (**a**) Plot of the lowest $^1S^e$ resonance energy E_r of π^- as a function of the screening parameter λ. (**b**) Plot of the corresponding resonance width Γ of π^- as a function of the screening parameter λ.
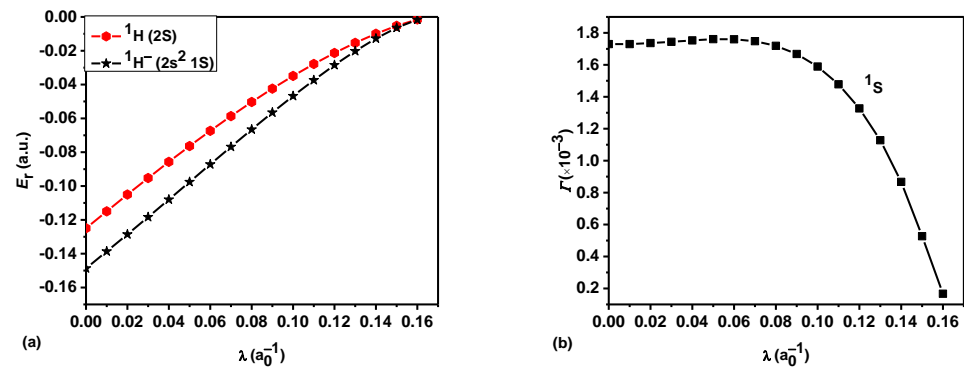
Figure 6. (**a**) Plot of the lowest $^1S^e$ resonance energy E_r of $^1H^-$ as a function of the screening parameter λ. (**b**) Plot of the corresponding resonance width Γ of $^1H^-$ as a function of the screening parameter λ.
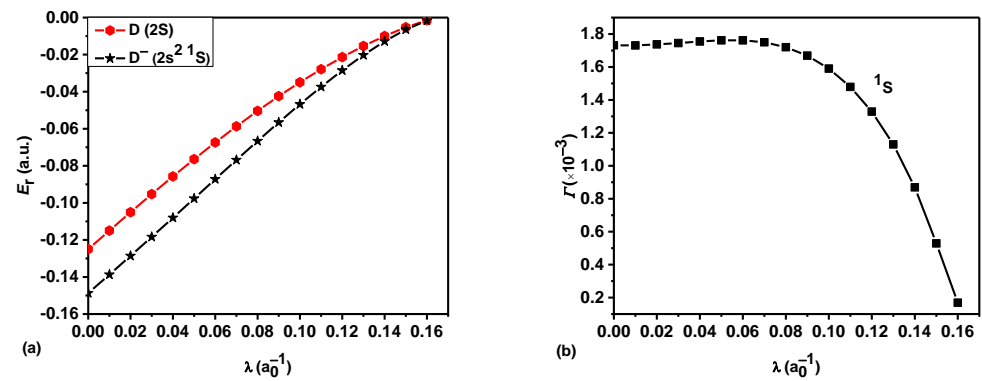
Figure 7. (**a**) Lowest $^1S^e$ resonance energy E_r of D^- versus λ. (**b**) Corresponding resonance width Γ of D^- versus λ.
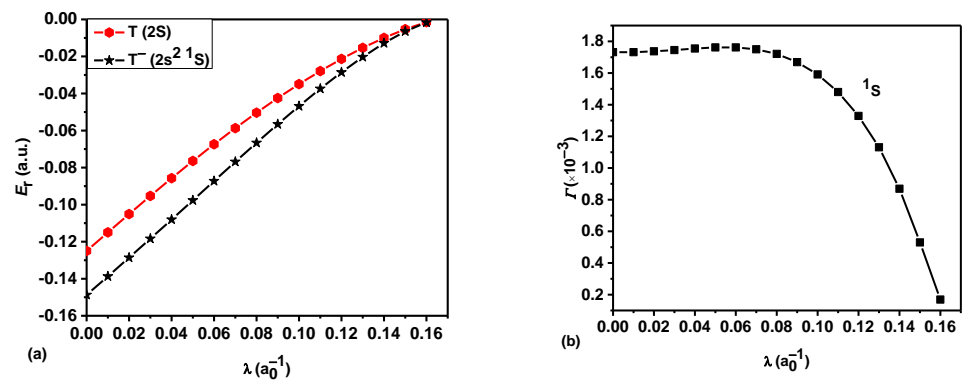
Figure 8. (**a**) Lowest $^1S^e$ resonance energy E_r of T^- as a function of λ. (**b**) Resonance width Γ of T^- as a function of λ.
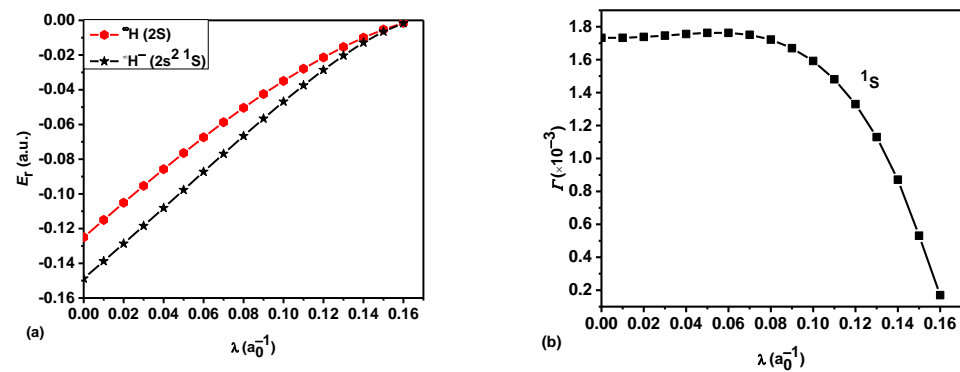
Figure 9. (**a**) Plot of the lowest $^1S^e$ resonance energy E_r of $^\infty H^-$ as a function of λ. (**b**) Plot of the corresponding resonance width Γ of $^\infty H^-$ as a function of λ.
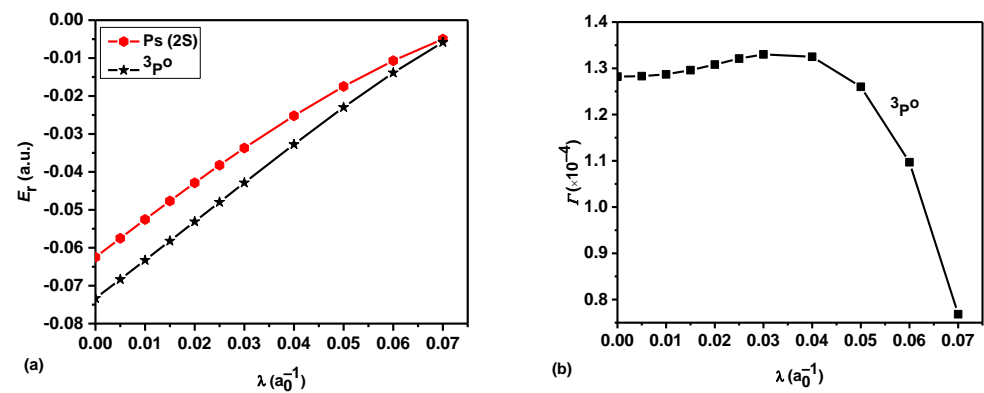
Figure 10. (**a**) Plot of the lowest $^3P^o$ resonance energy E_r of Ps^- as a function of the screening parameter λ. (**b**) Plot of the resonance width Γ of Ps^- as a function of the screening parameter λ.
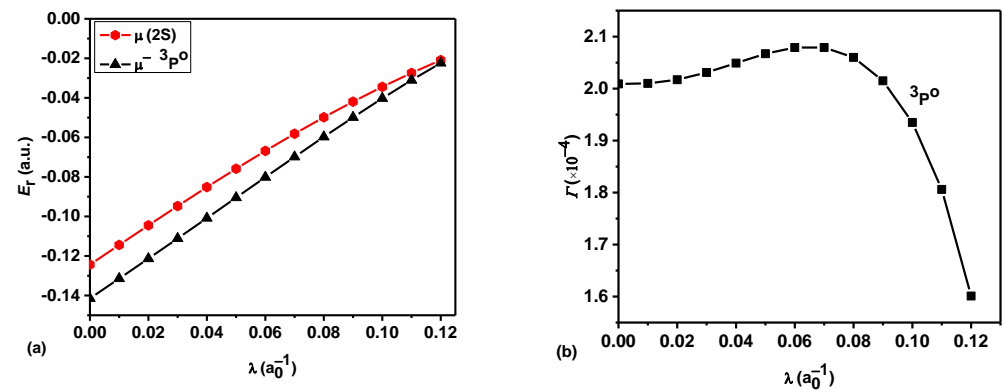
Figure 11. (**a**) Plot of the lowest $^3P^o$ resonance energy E_r of $M\mu^-$ vs. the screening parameter λ. (**b**) Plot of the corresponding resonance width Γ of $M\mu^-$ vs. the screening parameter λ.
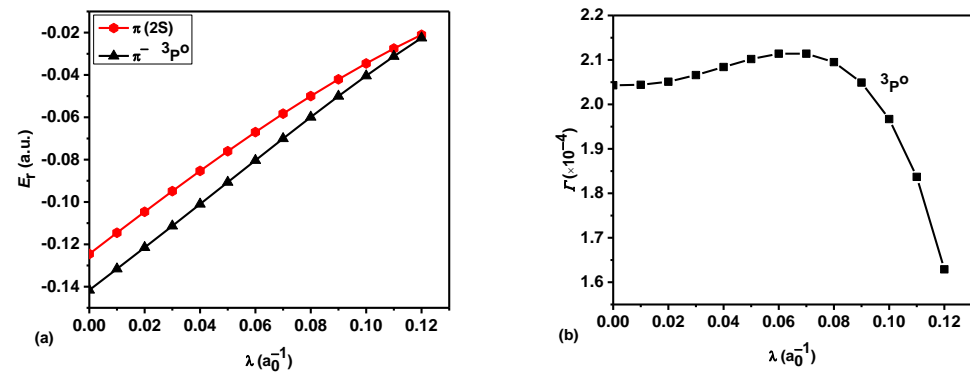
Figure 12. (**a**) Plot of the lowest $^3P^o$ resonance energy E_r of π^- as a function of λ. (**b**) Plot of the corresponding resonance width Γ of π^- as a function of λ.
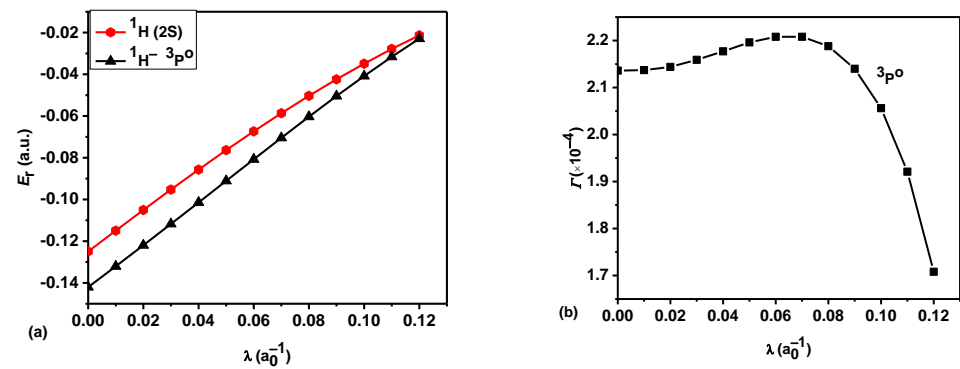
Figure 13. (**a**) Plot of the lowest $^3P^o$ resonance energy E_r of $^1H^-$ versus the screening parameter λ. (**b**) Plot of the corresponding resonance width Γ of $^1H^-$ versus λ.
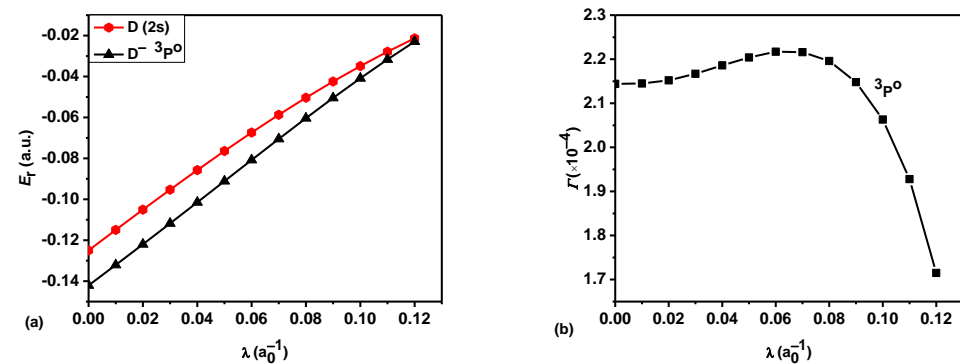
Figure 14. (**a**) Plot of the lowest $^3P^o$ resonance energy E_r of D^- vs. the screening parameter λ. (**b**) Plot of the corresponding resonance width Γ of D^- vs. the screening parameter λ.
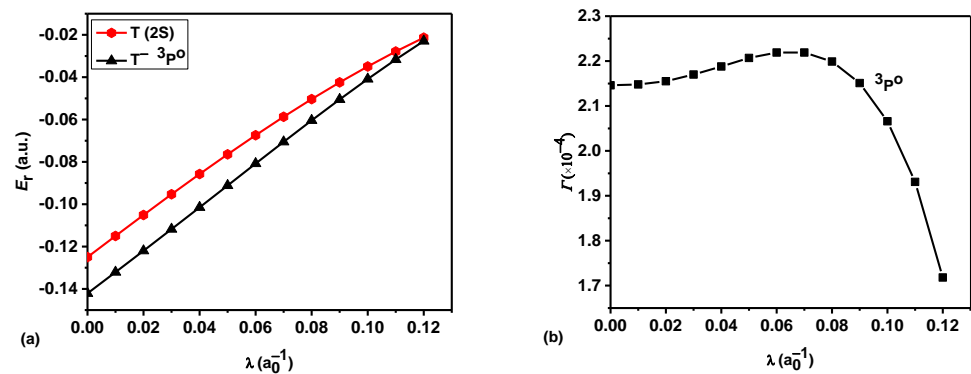
Figure 15. (**a**) Plot of the lowest $^3P^o$ resonance energy E_r of T^- vs. λ. (**b**) Plot of the corresponding resonance width Γ of T^- vs. λ.
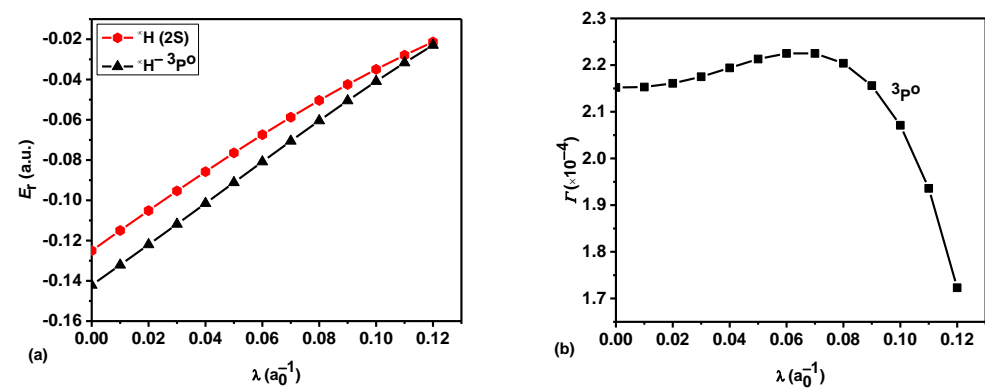
Figure 16. (**a**) Plot of the lowest $^3P^o$ resonance energy E_r of $^\infty H^-$ as a function of the screening parameter λ. (**b**) Plot of the corresponding resonance width Γ of $^\infty H^-$ as a function of the screening parameter λ.

4. Conclusions

This paper focused on the resonance states of negative hydrogen-like ions embedded in a quantum plasma medium. The correlated exponential wave function was chosen to solve the Schrödinger equation within the framework of a variational method. We used an exponential cosine screened Coulomb potential to model the effects of the quantum plasma environment on the proposed systems. The $^1S^e$ and $^3P^o$ resonance parameters (E_r, Γ) below the $N = 2$ threshold for the seven ions Ps^-, $M\mu^-$, π^-, $^1H^-$, D^-, T^- and $^\infty H^-$ for different screening parameters were accurately calculated by the stabilization method. We believe that the results obtained from the present theoretical investigation will provide valuable information for researchers in plasma physics, atomic–molecular physics, astrophysics and other related fields.

Author Contributions: S.Y., Z.J. and S.K. contributed equally to this work. All authors have read and agreed to the published version of the manuscript.

Funding: This research was funded by the Natural Science Foundation of Heilongjiang Province, grant number YQ2020A006.

Data Availability Statement: The data that supports the findings of this study are available within the article.

Conflicts of Interest: The authors declare no conflict of interest.

References

1. Wheeler, J.A. Polyelectrons. *Ann. N. Y. Acad. Sci.* **1946**, *48*, 219–238. [CrossRef]
2. Mills, A.P., Jr. Observation of the positronium negative ion. *Phys. Rev. Lett.* **1981**, *46*, 717–720. [CrossRef]

3. Mills, A.P., Jr. Measurement of the decay rate of the positronium negative ion. *Phys. Rev. Lett.* **1983**, *50*, 671–674. [CrossRef]
4. Ho, Y.K. Autoionization states of the positronium negative ion. *Phys. Rev. A* **1979**, *19*, 2347–2352. [CrossRef]
5. Ho, Y.K. Doubly excited resonances of positronium negative ions. *Phys. Lett. A* **1984**, *102*, 348–350. [CrossRef]
6. Botero, J. Adiabatic study of the positronium negative ion. *Phys. Rev. A* **1987**, *35*, 36–50. [CrossRef]
7. Ward, S.J.; Humberston, J.W.; McDowell, M.R.C. Elastic scattering of electrons (or positrons) from positronium and the photodetachment of the positronium negative ion. *J. Phys. B At. Mol. Phys.* **1987**, *20*, 127–149. [CrossRef]
8. Bhatia, A.K.; Ho, Y.K. Complex-coordinate calculation of ^{1,3}P resonances in Ps using Hylleraas functions. *Phys. Rev. A* **1990**, *42*, 1119–1122. [CrossRef]
9. Ho, Y.K.; Bhatia, A.K. ^{1,3}P^o resonance states in positronium ions. *Phys. Rev. A* **1991**, *44*, 2890–2894. [CrossRef]
10. Rost, J.M.; Wintgen, D. Positronium negative ion: Molecule or Atom? *Phys. Rev. Lett.* **1992**, *69*, 2499–2502. [CrossRef]
11. Ho, Y.K.; Bhatia, A.K. P-wave shape resonances in positronium ions. *Phys. Rev. A* **1993**, *47*, 1497–1499. [CrossRef]
12. Ho, Y.K. Doubly excited states of positronium negative ions. *Hyperfine Interact.* **1994**, *89*, 401–406. [CrossRef]
13. Igarashi, A.; Shimamura, I.; Toshima, N. Photodetachment cross sections of the positronium negative ion. *New J. Phys.* **2000**, *2*, 17. [CrossRef]
14. Basu, A.; Ghosh, A.S. Feshbach resonances in electron-positronium continuum and the close-coupling model. *Eur. Lett.* **2002**, *60*, 46–52. [CrossRef]
15. Li, T.; Shakeshaft, R. S-wave resonances of the negative positronium ion and stability of a system of two electrons and an arbitrary positive charge. *Phys. Rev. A* **2005**, *71*, 052505. [CrossRef]
16. Basu, A.; Ghosh, A.S. Doubly excited resonant states of positronium negative ion. *Phys. Rev. A* **2006**, *72*, 062507. [CrossRef]
17. Lin, C.H.; Ho, Y.K. Quantum Entanglement and Shannon Information Entropy for the doubly excited resonance state in positronium negative ion. *Atoms* **2015**, *3*, 422–432. [CrossRef]
18. Kar, S.; Wanga, Y.; Ho, Y.K. Triplet P states in Ps$^-$ using correlated exponential wave functions. *Chin. J. Phys.* **2020**, *68*, 137–146. [CrossRef]
19. Mills, A.P., Jr. Cross section for photoionization of the positronium negative ion at the lowest Feshbach resonance. *Can. J. Phys.* **2013**, *91*, 751–755. [CrossRef]
20. Nagashima, Y. Experiments on positronium negative ions. *Phys. Rep.* **2014**, *545*, 95–123. [CrossRef]
21. Mills, A.P., Jr. Possible experiments with high density positronium. *AIP Conf. Proc.* **2019**, *2182*, 030001.
22. Orr, N.A.; Ploszajczak, M.; Marqués, F.M.; Carbonell, J. *Recent Progress in Few-Body Physics: Proceedings of the 22nd International Conference on Few-Body Problems in Physics*; Springer: Cham, Switzerland, 2020; Volume 238.
23. Michishio, K.; Kanai, T.; Kuma, S.; Azuma, T.; Wada, K.; Mochizuki, I.; Hyodo, T.; Yagishita, A.; Nagashima1, Y. Observation of a shape resonance of the positronium negative ion. *Nat. Commun.* **2016**, *7*, 11060. [CrossRef] [PubMed]
24. Nagashima, Y.; Sakai, T. First observation of positronium negative ions emitted from tungsten surfaces. *New J. Phys.* **2006**, *8*, 319. [CrossRef]
25. Callaway, J. Energies and widths of the ^{1}P^o(1) and ^{1}S(2) resonant states of H$^-$. *Phys. Lett. A* **1978**, *68*, 315–316. [CrossRef]
26. Wendoloski, J.J.; Reinhardt, W.P. Effects of an external electric field on ^{1}P^o resonances of H$^-$. *Phys. Rev. A* **1978**, *17*, 195–200. [CrossRef]
27. Pathakt, A.; Kingston, A.E.; Berrington, K.A. Resonances in H$^-$ associated with the n = 2, 3 and 4 hydrogenic thresholds. *J. Phys. B At. Mol. Opt. Phys.* **1988**, *21*, 2939–2951. [CrossRef]
28. Ho, Y.K.; Bhatia, A.K. Doubly excited shape resonances in H$^-$. *Phys. Rev. A* **1993**, *48*, 3720–3724. [CrossRef]
29. Tang, J.Z.; Wakabayashi, Y.; Matsuzawa, M.; Watanabe, S.; Shimamura, I. Critical study of photodetachment of H$^-$ at energies up to the n = 4 threshold. *Phys. Rev. A* **1994**, *49*, 1021–1028. [CrossRef]
30. Lindroth, E. Photodetachment of H$^-$ and Li$^-$. *Phys. Rev. A* **1995**, *52*, 2737–2749. [CrossRef]
31. Zhou, Y.; Lin, C.D. Comparative studies of excitations and resonances in H$^-$, Ps$^-$, and e$^+$ + H systems. *Phys. Rev. Lett.* **1995**, *75*, 2296–2299. [CrossRef]
32. Chen, M.K. Doubly excited resonant states in H$^-$ below the n = 2 hydrogen threshold. *J. Phys. B At. Mol. Opt. Phys.* **1997**, *30*, 1669–1676. [CrossRef]
33. Gien, T.T. Feshbach resonances below the n = 2 H excitation threshold in electron–hydrogen scattering. *J. Phys. B At. Mol. Opt. Phys.* **1998**, *31*, L1001–L1008. [CrossRef]
34. Kuan, W.H.; Jiang, T.F. Photodetachment of H$^-$. *Phys. Rev. A* **1999**, *60*, 364–369. [CrossRef]
35. Bürgersa, A.; Lindroth, E. Doubly excited states in the negative hydrogen ion. *Eur. Phys. J. D* **2000**, *10*, 327–340. [CrossRef]
36. Jiao, L.G.; Ho, Y.K. Complete supermultiplet structures for the doubly excited intrashell resonances of H$^-$ associated with the H (N = 2, 3 and 4) thresholds. *Phys. Rev. A* **2014**, *89*, 052511. [CrossRef]
37. Hamm, M.E.; Hamm, R.W.; Donahue, J.; Gram, P.A.M.; Pratt, J.C.; Yates, M.A.; Bolton, R.D.; Clark, D.A.; Bryant, H.C.; Frost, C.A.; et al. Observation of narrow resonances in the H photodetachment cross section near the n = 3 Threshold. *Phys. Rev. Lett.* **1979**, *43*, 1715–1718. [CrossRef]
38. Halka, M.; Bryant, H.C.; Mackerrow, E.P.; Miller, W.; Mohagheghi, A.H.; Tang, C.Y.; Cohen, S.; Donahue, J.B.; Hsu, A.; Quick, C.R.; et al. Observation of the partial decay into H^0 (n$'$ = 2) by excited H$^-$ near the n = 3 and 4 thresholds. *Phys. Rev. A* **1991**, *44*, 6127–6129. [CrossRef]
39. Buckman, S.J.; Clark, C.W. Atomic negative-ion resonances. *Rev. Mod. Phys.* **1994**, *66*, 539. [CrossRef]

40. Balling, P.; Andersen, H.H.; Brodie, C.A.; Pedersen, U.V.; Petrunin, V.V.; Raarup, M.K.; Steiner, P.; Andersen, T. High-resolution VUV spectroscopy of H$^-$ in the region near the H (n = 2) threshold. *Phys. Rev. A* **2000**, *61*, 022702. [CrossRef]

41. Ross, T.; Baker, E.J.; Snow, T.P.; Destree, J.D.; Rachford, B.L.; Drosback, M.M.; Jensen, A.G. The search for H$^-$ in astrophysical environments. *Astrophys. J.* **2008**, *684*, 358–363. [CrossRef]

42. Kuang, Y.; Arnold, K.-P.; Chmely, F.; Eckhause, M.; Hughes, V.W.; Kane, J.R.; Kettell, S.; Kim, D.-H.; Kumar, K.; Lu, D.C.; et al. First observation of the negative muonium ion produced by electron capture in a beam-foil experiment. *Phys. Rev. A* **1987**, *35*, 3172–3175. [CrossRef] [PubMed]

43. Frolov, A.M. A discretisation of the Laplace transformation and an accurate method for the Coulomb three-body problem. *Z. Phys. D At. Mol. Clust.* **1986**, *2*, 61–65. [CrossRef]

44. Petelenz, P.; Smith, V.H., Jr. Binding energies of the muonium and positronium negative ions. *Phys. Rev. A* **1987**, *36*, 5125–5126. [CrossRef] [PubMed]

45. Bhatia, A.K.; Drachman, R.J. Three-body Coulomb bound states. *Phys. Rev. A* **1987**, *35*, 4051–4054. [CrossRef] [PubMed]

46. Frolov, A.M. Bound-state properties of negatively charged hydrogenlike ions. *Phys. Rev. A* **1998**, *58*, 4479–4483. [CrossRef]

47. Kar, S.; Ho, Y.K. Ground state and resonance state of Ps$^-$ in plasmas with various Debye lengths. *Phys. Rev. A* **2005**, *71*, 052503. [CrossRef]

48. Kar, S.; Ho, Y.K. Doubly excited ^{1,3}P^o resonance states of Ps$^-$ in weakly coupled plasmas. *Phys. Rev. A* **2006**, *73*, 032502. [CrossRef]

49. Basu, A.; Ghosh, A.S. Electron–positronium scattering in Debye plasma environment. *Nucl. Instrum. Methods Phys. Res. B* **2008**, *266*, 522–525. [CrossRef]

50. Kar, S.; Ho, Y.K. Photodetachment of the positronium negative ion interacting with screened Coulomb (Yukawa) potentials. *Few-Body Syst.* **2008**, *42*, 73–81. [CrossRef]

51. Ho, Y.K.; Kar, S. Complex-scaling calculations for doubly excited resonances in Ps$^-$ interacting with screened Coulomb (Yukawa) potentials. *Few-Body Syst.* **2012**, *53*, 437–443. [CrossRef]

52. Ho, Y.K.; Kar, S. High-lying doubly excited resonances in Ps$^-$ interacting with screened Coulomb potentials. *Chin. J. Phys.* **2016**, *54*, 574–581. [CrossRef]

53. Ho, Y.K. The combined screened Coulomb and varying charge effects on doubly excited resonance states in the positronium negative ion. *JPS Conf. Proc.* **2017**, *18*, 011027.

54. Kar, S.; Ho, Y.K. Autoionizing ^{1}S^e resonance of H$^-$ in Debye plasma environments. *Phys. Rev. E* **2004**, *70*, 066411. [CrossRef] [PubMed]

55. Kar, S.; Ho, Y.K. Electron affinity of the hydrogen atom and a resonance state of the hydrogen negative ion embedded in Debye plasmas. *New J. Phys.* **2005**, *7*, 141. [CrossRef]

56. Kar, S.; Ho, Y.K. Doubly-excited ^{1,3}P^o states of H$^-$ interacting with screened Coulomb (Yukawa) potentials. *Few-Body Syst.* **2006**, *40*, 13–20. [CrossRef]

57. Shukla, P.K.; Eliasson, B. Screening and wake potentials of a test charge in quantum plasmas. *Phys. Lett. A* **2008**, *372*, 2897–2899. [CrossRef]

58. Ghoshal, A.; Ho, Y.K. Properties of the positronium negative ion interacting with exponential cosine-screened Coulomb potentials. *Few-Body Syst.* **2009**, *46*, 249–256. [CrossRef]

59. Ghoshal, A.; Ho, Y.K. Autoionization states of the positronium negative ion in exponential cosine-screened Coulomb potentials. *Eur. Phys. J. D* **2010**, *56*, 151–156. [CrossRef]

60. Ghoshal, A.; Ho, Y.K. Properties of hydrogen molecular ion with static screened Coulomb and exponential cosine screened Coulomb potentials. *Int. J. Quantum Chem.* **2011**, *111*, 4288–4295. [CrossRef]

61. Ghoshal, A.; Ho, Y.K. Ground states and doubly excited resonance states of H$^-$ embedded in dense quantum plasmas. *J. Phys. B At. Mol. Opt. Phys.* **2009**, *42*, 175006. [CrossRef]

62. Kar, S.; Ho, Y.K. Excitons and the positronium negative ion: Comparison of spectroscopic properties. In *Excitons*; Pyshkin, S.L., Ed.; Intech: London, UK, 2018; pp. 69–90.

63. Mohr, P.J.; Newell, D.B.; Taylor, B.N. CODATA recommended values of the fundamental physical constants: 2014. *J. Phys. Chem. Ref. Data* **2016**, *45*, 043102. [CrossRef]

64. Bhattacharyya, S.; Saha, J.K.; Mukherjee, P.K.; Mukherjee, T.K. Three-body negative ions under Coulomb interaction. *Phys. Scr.* **2012**, *85*, 065305. [CrossRef]

65. Frolov, A.M. Multibox strategy for constructing highly accurate bound-state wave functions for three-body systems. *Phys. Rev. E* **2001**, *64*, 036704. [CrossRef]

66. Mandelshtam, V.A.; Ravuri, T.R.; Taylor, H.S. Calculation of the density of resonance states using the stabilization method. *Phys. Rev. Lett.* **1993**, *70*, 1932–1935. [CrossRef]

67. Kar, S.; Ho, Y.K. S-wave resonances in e$^+$ − He scattering below the Ps (n = 2) excitation threshold. *J. Phys. B At. Mol. Opt. Phys.* **2004**, *37*, 3177–3186. [CrossRef]

68. Ho, Y.K.; Bhatia, A.K.; Temkin, A. Precision calculation of the lowest ^{1}S resonance in e-H scattering. *Phys. Rev. A* **1977**, *15*, 1423–1429. [CrossRef]

69. Bhatia, A.K.; Pesnell, W.D. A note on the opacity of the Sun's atmosphere. *Atoms* **2020**, *8*, 37. [CrossRef]

70. Ghoshal, A.; Ho, Y.K. Photodetachment of H$^-$ in dense quantum plasmas. *Phys. Rev. E* **2010**, *81*, 016403. [CrossRef]

71. Ghoshal, A.; Ho, Y.K. Photodetachment of the positronium negative ions with exponential cosine-screened Coulomb potentials. *Few-Body Syst.* **2010**, *47*, 185–192. [CrossRef]
72. Jung, A.D. Resonant Compton scattering in nonthermal astrophysical plasmas. *Astrophys. J.* **2009**, *695*, 917–920. [CrossRef]
73. Li, H.W.; Kar, S. Plasma screening effects on resonant Compton scattering of photons by excited hydrogenic ions in Lorentzian plasmas. *Eur. Phys. J. D* **2012**, *66*, 304. [CrossRef]